Stomatin is a major lipid-raft component of platelet α granules

Mario Mairhofer, Marianne Steiner, Wilhelm Mosgoeller, Rainer Prohaska, and Ulrich Salzer

Lipid rafts are detergent-resistant, cholesterol- and sphingolipid-rich membrane domains that are involved in important cellular processes such as signal transduction and intracellular trafficking. Stomatin, a major lipid-raft component of erythrocytes and epithelial cells, is also an abundant platelet protein. Microscopical methods and subcellular fractionation showed that stomatin is located mainly at the α-granular membrane. The lipid-raft marker proteins flotillin-1 and flotillin-2 were also present in platelets but excluded from α granules. Stomatin and the flotillins were associated with Triton X-100–insoluble lipid rafts. Whereas stomatin was partly soluble in Triton X-100, it was insoluble in the detergents Lubrol and 3-[(3-cholamidopropyl)dimethylamonio]-1-propyl sulfonate (CHAPS). Flotation experiments after CHAPS lysis of platelets revealed a distinct set of lipid-raft–associated proteins, which were identified by matrix-assisted laser desorption/ionization mass spectrometry as stomatin, flotillin-1, flotillin-2, CD36, CD9, integrin $\alpha_{IIb}\beta_3$, and the glucose transporter GLUT-3. Stomatin, the flotillins, and CD36 were exclusively present in this lipid-raft fraction. Activation of platelets by calcium ionophore A23187 or thrombin led to translocation of stomatin to the plasma membrane, cleavage by calpain, and specific sorting into released microvesicles. In conclusion, this study demonstrated the existence of α-granular lipid rafts and suggests an important role for stomatin in the organization and function of α granules. (Blood. 2002;100:897-904)

© 2002 by The American Society of Hematology

Introduction

Stomatin (protein 7.2b, band 7.2), described as a major protein component of the erythrocyte membrane,[1-4] has been found to be absent from red cell membranes in patients with overhydrated hereditary stomatocytosis.[4,5] However, because normal stomatin messenger RNA is present in the reticulocytes[6] of these patients and stomatocytosis does not occur in stomatin knockout mice,[7] the absence of stomatin is an effect rather than the cause of the disease. Studies in UAC epithelial cells revealed that stomatin forms high-order oligomers and is associated with detergent-resistant membrane microdomains, which are also termed lipid rafts.[8,9] These characteristics of stomatin and its unusual monotopic structure[10] are reminiscent of typical features of the caveolin proteins, which are highly enriched at the cytoplasmic side of caveolae. In erythrocytes, which do not express caveolins, stomatin and the distantly related proteins flotillin-1 and flotillin-2[11] are the major integral membrane proteins of lipid rafts, suggesting important, yet distinct roles for these proteins at the interface between lipid rafts and the cytoskeleton or signaling components.[12]

The concept of lipid rafts or membrane microdomains was originally proposed to explain the vectorial transport of glycosyl phosphatidylinositol (GPI)–anchored proteins to the apical surface in polarized cells.[13,14] In the past decade, numerous studies have established the general characteristics of lipid rafts.[15-18] These microdomains contain mainly cholesterol and sphingolipids as lipid constituents, which make them insoluble in nonionic detergents, and are specifically enriched in different sets of proteins, namely, GPI-anchored proteins such as Thy-1 and PrP; palmitoylated proteins such as G proteins, Src family kinases, and caveolins; tetraspanin proteolipids; and other signaling proteins. However, lipid rafts are heterogeneous in their specific lipid and protein content, and different types of rafts coexist at the plasma membrane, even within close proximity. This was first shown by Schnitzer et al,[19] who separated caveolae, which are morphologically and functionally distinct lipid microdomains of the plasma membrane, from associated lipid rafts, which contain the bulk of GPI-linked proteins.

Recently, confocal microscopy and biochemical analysis of the marker proteins prominin and placental alkaline phosphatase revealed 2 distinct lipid microdomains in the microvilli of Madin-Darby canine kidney cells.[20] Moreover, a structural diversity of lipid rafts occupied by functionally different GPI-linked proteins has been observed at the plasma membrane of neurons.[21] However, lipid rafts are present not only at the plasma membrane but are also found at internal membranes of the secretory[14] or endocytic[22] pathways and at other intracellular organelles, such as the Golgi complex[23] and the phagosomes.[24] Hence, lipid rafts appear to be involved in the complex network of intracellular membrane trafficking, an idea that is supported by the various subcellular localizations of a specific lipid-raft protein, depending on the cell type and state of differentiation.[23-26]

Platelets are anuclear secretory blood cells that contain a complex network of membrane structures, including the plasma membrane, the α granules, dense granules, the surface-connected canalicular system (SCCS), and the dense tubular system. The existence of platelet lipid rafts was previously described, with the glycoprotein (GP) CD36 and active Lyn tyrosine kinase found to be

© 2002 by The American Society of Hematology

greatly enriched and GPIb, integrin β_3 (CD61), CD9, and actin observed to be partly present in the Triton X-100 (TX-100)–insoluble membrane domains.[27,28] However, nothing is known about the subcellular localization of these rafts within the platelet membrane system, since none of the identified raft proteins is restricted to only one type of membrane. Immunoelectron microscopy revealed that a considerable pool of the plasma membrane proteins CD36, GPIb (CD42b), integrin $\alpha_{IIb}\beta_3$ (GPIIb-IIIa also known as CD41/CD61) and CD9 is present in the α granules, probably because of a clathrin-based endocytic sorting process that occurs not only in megakaryocytes but also in mature resting platelets.[29-32] Lyn and other Src family kinases are found predominantly at these endocytotic vesicles, thus suggesting a role for them in trafficking of plasma proteins to the α granules.[33]

In this study, we showed that stomatin is an abundant platelet protein located at the α-granular membrane. We found that stomatin is present in lipid rafts, thereby proving that rafts exist in α granules. On thrombin activation, stomatin translocated to the plasma membrane and became selectively enriched in released microvesicles. Compared with stomatin, the flotillins had a different subcellular localization in resting platelets and were essentially depleted from microvesicles on thrombin activation. Our study revealed different types of platelet lipid rafts and suggests an important role for them in the intracellular membrane system.

Materials and Methods

Chemicals

Protease inhibitors aprotinin, pepstatin A, leupeptin, phenylmethylsulfonyl fluoride (PMSF), calcium ionophore A23187, thrombin, methyl-β-cyclodextrin (mβCD), and the detergents TX-100, 3-[(3-cholamidopropyl)dimethylamonio]-1-propyl sulfonate (CHAPS), octyl glucoside (OG), and Nonidet P-40 (NP-40) were purchased from Sigma (St Louis, MO). Lubrol 17A17 was obtained from Serva (Heidelberg, Germany), the calpain inhibitor (2S,3S)-trans-epoxysuccinyl-L-leucylamido-3-methylbutane ethyl ester (E-64d) was from Sigma, calpeptin (N-benzyloxycarbonyl-L-leucylnorleucinal) was from Calbiochem (San Diego, CA), and the calpain inhibitor peptide (DPMSSTYIEELGKREVTIPPKYRELLA) was from BioSource (Nivelles, Belgium). The D_C protein assay kit was from BioRad (Hercules, CA), and the enzymatic cholesterol determination kit was from Roche Diagnostics (Mannheim, Germany).

Antibodies

Monoclonal antibodies to flotillin-2 (epidermal surface antigen), flotillin-1, and clathrin (heavy chain) were purchased from Transduction Laboratories (San Diego, CA); monoclonal antibodies to spectrin, β-actin, and α-tubulin, and goat polyclonal antibody to von Willebrand factor (VWF) were from Sigma; and polyclonal antibodies to Lyn, GPIb (CD42b), CD36, and P-selectin were from Santa Cruz Biotechnologies (Santa Cruz, CA). Monoclonal antibodies to stomatin (GARP-50 and GARP-61) were described previously.[33] GARP-50 was used for immunoelectron and light microscopy experiments and for Western blotting, and GARP-61 was used for Western blotting only. For blocking GARP-50 in microscopical studies, we used an N-terminal peptide of stomatin (residues 1-24) containing the epitope.

Identification of proteins

Proteins were analyzed by sodium dodecyl sulfate–polyacrylamide gel electrophoresis (SDS-PAGE) and silver staining.[33] Protein bands were excised, digested with trypsin, and identified by mass spectrometry (Bruker Reflex III matrix-assisted laser desorption/ionization time-of-flight mass spectrometry [MALDI-TOF-MS]; Bruker Daltonics, Billerica, MA). The identity of the respective proteins was confirmed by Western blotting.

Immunostaining for light microscopy

For stomatin immunofluorescence staining on blood and bone marrow smears, cells were fixed in methanol at 4°C for 10 minutes, treated with 0.5% TX-100 in phosphate-buffered saline (PBS; pH 7.3) for 3 minutes at 4°C, and washed 3 times in PBS for 5 minutes each time. Blocking of unspecific binding sites and the staining protocol were carried out as described previously.[34] The primary anti–stomatin antibody incubation was performed with the monoclonal antibody GARP-50 hybridoma supernatant, used either undiluted or diluted 1:3 with preincubation buffer, for 1 hour. Slides were examined and photographed with black and white film by using a Leitz fluorescence microscope.

For immunocytochemistry, the cells were extracted with 0.5% TX-100 in PBS (pH 7.3) at 4°C for 3 minutes or 30 minutes and washed 3 times in PBS. The primary antibodies were detected by using the Chem-Mate horseradish peroxidase–diaminobenzidine system designed for automated immunostaining (DAKO, Glostrup, Denmark) with one modification. To improve the blocking, we used 3% hydrogen peroxide in 50% methanol for 3 minutes at room temperature to suppress endogenous peroxidase activity completely. After signal detection, the slides were dehydrated in ethanol and xylene and mounted with Eukitt (Merck, Darmstadt, Germany). Cells were photographed with a Nikon Mikrophot FX4 with black and white film.

Immunoelectron microscopy

Platelets were isolated from whole blood by density-gradient centrifugation through Lymphoprep (Nygaard, Denmark) and washed in PBS. For activation, platelets were incubated with 1 μM calcium ionophore A23187, as described previously.[35] Resting or activated platelets were fixed for 30 minutes in 2% freshly depolymerized formaldehyde, washed, embedded, and sectioned as described previously.[36] The sections were preincubated with PBS containing 5% bovine serum albumin and 0.5% Tween-20 (PBS-ST) for blocking of unspecific binding sites, and this was followed by incubation with monoclonal antibody GARP-50 at 22°C for 1 hour. The grids were rinsed 3 times, incubated with anti–mouse IgG linked to 10 nm colloidal gold (Biocell, Cardiff, United Kingdom) diluted 1:40 in PBS-ST (pH adjusted to 8.0), rinsed, counterstained, and examined as described previously.[36]

For controls, we omitted the primary antibody or preabsorbed the specific antibody by incubation with a 100 to 1000 times molar excess of the N-terminal stomatin peptide for 20 minutes at 37°C. Both procedures abolished specific signal at the light and electron microscopical levels.

While inspecting immunostained platelets, we recognized an increased cell-membrane labeling in activated platelets. To objectify this impression by morphometry on electron micrographs, we determined the grain density along the cell membrane (gold grains per membrane-length unit) in 10 resting and in 13 activated platelets and compared the 2 groups by using the Student t test.

Isolation of platelets

Whole blood (45 mL) was obtained from healthy donors by venipuncture and collected into heparin-treated tubes. Red cells and leukocytes were formed into pellets (by centrifugation at $200g$ for 15 minutes), the platelet-rich plasma was removed from the tubes, and 9 parts were mixed with 1 part acid-citrate-dextrose solution (25 g/L trisodium [Na$_3$] citrate, 13.7 g/L citric acid, and 20 g/L glucose) as an anticoagulant. Platelets from this mixture were formed into pellets ($2000g$ for 12 minutes) and resuspended in washing buffer (90 mM sodium chloride [NaCl], 5 mM potassium chloride [KCl], 36 mM Na$_3$ citrate, and 10 mM EDTA). This washing step was repeated, remaining erythrocytes were removed by 1 or 2 quick spins, and the final platelet pellet was resuspended in the appropriate buffer for the various experiments. Buffer I (134 mM NaCl, 12 mM sodium bicarbonate, 2.9 mM KCl, 0.34 mM sodium phosphate dibasic, 1 mM magnesium chloride, 10 mM HEPES, and 5 mM glucose [pH 7.4]) was used for platelet homogenization. Buffer I containing 2 mM calcium chloride (CaCl$_2$) was used for microvesicle isolation, calpain-inhibition experiments, flotation assays, and solubilization experiments. Typical platelet counts ranged from 0.5 to 2.0×10^9 cells/mL.

Platelet homogenization and fractionation

The platelets obtained from individual donors were resuspended in 1 mL buffer I (1-2 × 10⁹ cells/mL) and mixed with 1 mL precooled 2 × Tris–citrate buffer (126 mM Tris-Cl, 190 mM NaCl, 10 mM KCl, and 24 mM citric acid [pH 6.5]) containing 2 mM PMSF, 2 μg/mL pepstatin A, 20 μg/mL leupeptin, and 20 μg/mL aprotinin. The platelet suspension was put on ice and homogenized in an Aminco French pressure cell (210 930 kg/m²). The platelet lysate was centrifuged (2000g for 10 minutes at 4°C) to obtain pellets of unhomogenized platelets. The supernatant was laid on top of a linear sucrose density gradient (30%-60% sucrose, 10 mM Tris-Cl, 150 mM NaCl, and 5 mM EDTA [pH 7.4]) and centrifuged (200 000g for 2 hours at 4°C) in an SW 40 rotor (Beckman Coulter, Fullerton, CA). Eighteen fractions (700 μL each) were collected from the top of the gradient, and the pellet at the bottom was resuspended in the 18th fraction. Aliquots from each fraction were mixed with reducing or nonreducing SDS-PAGE sample buffer, boiled for 3 minutes, and loaded on 11% polyacrylamide gels for analysis by Western blotting or silver staining.

Preparation of lipid rafts

Platelet pellets were resuspended in buffer I containing 2 mM CaCl₂ (0.5-2 × 10⁹ cells/mL) and lysed by addition of an equal volume of ice-cold TX-100 lysis buffer (2% TX-100, 100 mM Tris-Cl, 10 mM EGTA, 2 mM PMSF, 2 μg/mL pepstatin A, 20 μg/mL leupeptin, and 20 μg/mL aprotinin [pH 7.4]) or ice-cold CHAPS lysis buffer (TX-100 replaced by 2% CHAPS). The final detergent concentration was 1%, and lysates were mixed carefully and kept at 4°C for 20 minutes. The protein concentration ranged from 1.5 to 5.3 mg/mL. Subsequently, the lysates were mixed with 80% sucrose in Tris-buffered saline (TBS; 10 mM Tris-Cl and 150 mM NaCl [pH 7.4]) containing 1% TX-100 or 1% CHAPS to yield a final sucrose concentration of 50%. Then, 750 μL of the 50% sucrose layer was pipetted into SW 50 centrifuge tubes and overlaid with 750 μL each of 40%, 30%, 20%, and 10% sucrose in TBS [pH 7.4]. These sucrose step gradients were centrifuged in a precooled Beckman SW 50.1 rotor for 17 hours (230 000g at 4°C). Lipid rafts were visible as whitish bands at the 10% to 20% sucrose interface. Five fractions of 750 μL were collected from the top of the gradient, and the pellet at the bottom of the tube was resuspended in 750 μL TBS (pH 7.4). Aliquots of the fractions were mixed with SDS-PAGE sample buffer and boiled for 3 minutes. Equal volumes of the fractions were loaded on the gels and analyzed by Western blotting and silver staining as described previously.[33] For silver staining, fraction 5, which contained by far the most protein, was diluted 1:10 with SDS-PAGE sample buffer.

In one experiment, platelets resuspended in buffer I containing 2 mM CaCl₂ were treated with 0.5% mβCD (final concentration) for 30 minutes at 37°C. Platelet lysis and subsequent density-gradient centrifugation was done as described above.

Solubilization experiments

Platelets were resuspended in 0.5 mL buffer I containing 2 mM CaCl₂ (2 × 10⁹ cells/mL), and 100-μL aliquots were lysed by addition of 100 μL ice-cold lysis buffer containing the following detergents to yield the final concentrations indicated in parentheses: Lubrol (1%), CHAPS (1%), TX-100 (1%), OG (60 mM), and NP-40 (1%). The mixtures were incubated at 4°C for 20 minutes. Subsequently, insoluble material was formed into pellets by centrifugation (100 000g for 1 hour at 4°C). The pellet was resuspended in 200 μL of a mixture of equal volumes buffer I containing 2 mM CaCl₂ and lysis buffer. The pellet and supernatant samples were mixed with SDS-PAGE sample buffer and boiled for 3 minutes. Equal volumes of these samples were analyzed by Western blotting.

Isolation of microvesicles

Platelets were resuspended in buffer I containing 2 mM CaCl₂ (1-2 × 10⁹ cells/mL) and activated by 4 μM calcium ionophore A23187 or 1 U/mL thrombin on a shaker for 30 minutes at 37°C. EDTA was added to produce a final concentration of 5 mM, and the platelet suspensions were centrifuged (2000g for 10 minutes) to form the platelets into pellets. The platelet pellets were resuspended in buffer I containing 5 mM EDTA. Microvesicles were formed into pellets from the supernatant (10 000g for 30 minutes at 4°C[37]), resuspended in buffer I containing 5 mM EDTA, centrifuged (2000g for 10 minutes) to remove contaminating platelets, formed into pellets again, and resuspended in buffer I containing 5 mM EDTA. The protein content of the corresponding platelet and microvesicle suspensions was determined with the D_C protein assay, and equal protein amounts of platelets and microvesicles were analyzed by SDS-PAGE and Western blotting.

Identification of calpain-cleavage products after platelet activation

Platelets were resuspended in buffer I containing 2 mM CaCl₂ (1 × 10⁹ cells/mL). Aliquots (0.1 mL) of the platelet suspension were mixed with 1 μL of a 5 mg/mL dimethyl sulfoxide solution of the membrane-permeable calpain inhibitors E-64d[38] and calpeptin,[39] respectively, and incubated at 37°C for 30 minutes. Preincubated samples and respective controls were then activated by adding calcium ionophore A23187 (4 μM final concentration) at 37°C for 20 minutes. The samples were analyzed by SDS-PAGE and Western blotting.

Results

To identify blood cells that express stomatin, we used the GARP-50 monoclonal antibody, which recognizes an N-terminal epitope of stomatin, for immunocytochemical staining. In smear preparations, platelets revealed the highest signal density of all blood cells (Figure 1A). Typically, the label distribution was heterogeneous, with most of the signal concentrated in the center of the platelets. It consistently revealed a granular pattern that was easier to recognize with immunofluorescence microscopy (Figure 1B) than with immunocytochemistry (Figure 1A). Considerably less staining was observed over the periphery of the platelets. Megakaryocytes in bone marrow smears had intense and heterogeneous labeling after GARP-50 immunofluorescence staining (Figure 1C). Immunoelectron microscopy of resting platelets revealed that most of the immunogold grains were located at the membrane of the α granules (Figure 1D). Activated platelets could be recognized by their granule morphologic features and cytoplasmic protrusions leading to an irregularly shaped circumference (Figure 1E). Activated platelets had a significantly higher label density over the plasma membrane ($P < .02$ on 2-tailed Student t test). The cell-membrane label density on electron micrographs of resting platelets was found to be 0.11 ± 0.098 (mean ± SE; n = 10) gold grains/μm; for activated platelets, the density was 0.23 ± 0.115 (n = 13) gold grains/μm. This indicates that stomatin is translocated to the plasma membrane during the activation and degranulation of platelets (also compare Figure 1D and 1E).

To examine the subcellular localization of stomatin more closely, we analyzed platelet homogenates by using linear sucrose density-gradient centrifugation to separate the different platelet organelles from the bulk of cytosolic and plasma membrane proteins.[40] Western blot analysis of the gradient fractions revealed 2 distinct pools of stomatin (Figure 2). Stomatin was partly present in the low-density fractions, which contained most of the cytoplasmic and plasma membrane proteins, and in fractions of higher densities (∼ 50% sucrose), in which intracellular granules are expected. This distribution was paralleled by P-selectin and VWF, 2 marker proteins of α granules, indicating the association of stomatin with these granules. The presence of a minor amount of the α-granule markers in the low-density fractions can be explained by a partial rupture of the granules during homogenization. As expected, the
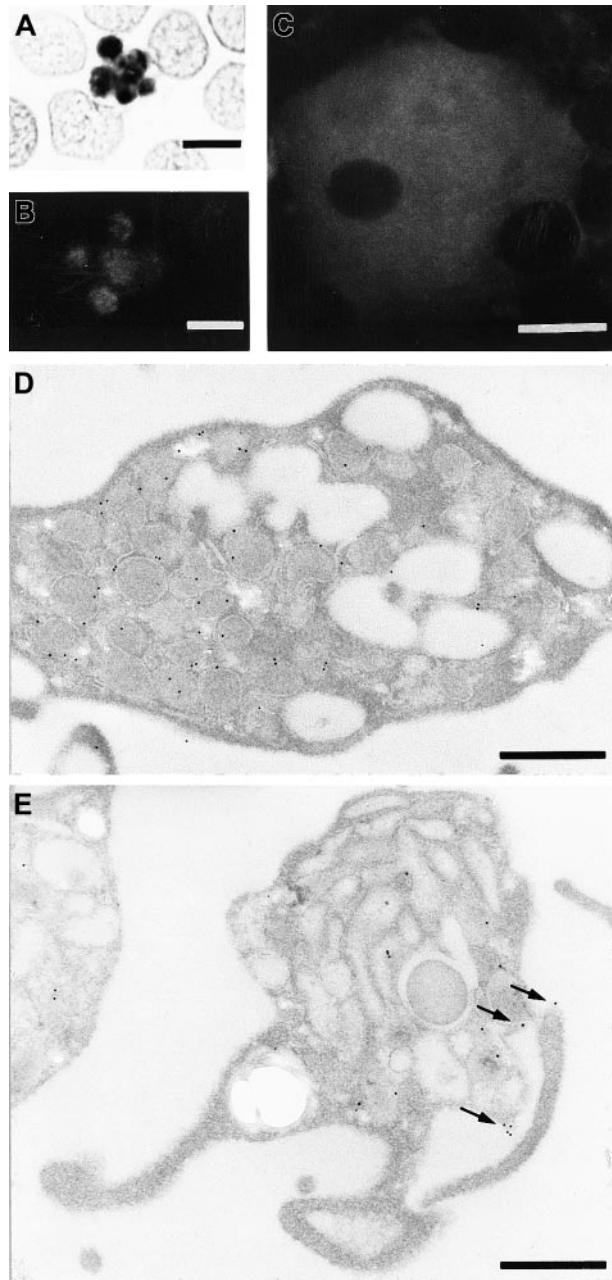
Figure 1. Immunolocalization of stomatin to platelets and megakaryocytes. A blood smear was analyzed to identify stomatin in platelets by immunocytochemistry with diaminobenzidine as substrate following 30 minutes of cell extraction with TX-100 (A) and immunofluorescence microscopy following 3 minutes of TX-100 extraction (B). Immunoreactivity in the central granule membranes is intense, leaving less signal in the peripheral cytoplasm of the platelets. (C) Identification of stomatin in a megakaryocyte from bone marrow, as observed with immunofluorescence. The nucleus is free of labeling, and the cytoplasm is stained almost homogeneously, with some patches of increased cytoplasmic signal. Immunoelectron microscopy of resting platelets (D) and activated platelets (E) revealed the subcellular localization of stomatin. In resting platelets, the labeling is predominantly over the membrane of α granules (D), whereas in activated platelets, the plasma membrane is consistently labeled in addition to the granular membrane (arrows in E). Bars represent 5 μm (A and B), 10 μm (C), or 0.5 μm (D and E).

major platelet-surface antigen GPIb (CD42b) was found predominantly in the low-density fractions. The lipid-raft marker proteins flotillin-1 and flotillin-2 were present in platelets but showed a subcellular distribution different from that of stomatin (Figure 2). Flotillins were not present in α granules but were restricted to the plasma membrane or other light membranes.
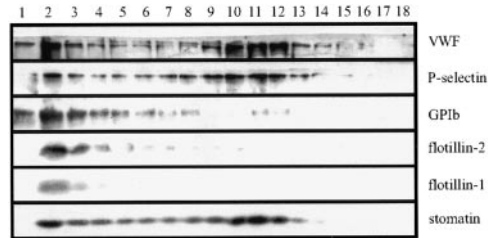

Figure 2. Stomatin codistributes with α-granular marker proteins on sucrose density gradients. Platelet homogenates (1×10^9 cells/mL) were separated by sucrose density-gradient (30%-60%) centrifugation. Eighteen fractions were collected (starting from the top), and aliquots were analyzed by SDS-PAGE and Western blotting. Representative data are shown (n = 5).

Because of the association of stomatin with lipid rafts in a variety of cells, we wanted to know whether stomatin is also present in platelet lipid rafts. To isolate lipid rafts, platelets were lysed in TX-100 on ice and subjected to discontinuous density-gradient centrifugation. The Western blot analysis shown in Figure 3A demonstrates that stomatin and the flotillin proteins were partly present in the low-density fractions, together with the Lyn protein. The most abundant proteins of the lipid-raft fractions (fractions 1-3), as shown on silver staining, were analyzed by MALDI-TOF-MS and identified as stomatin, actin, and CD36 (Figure 3A).
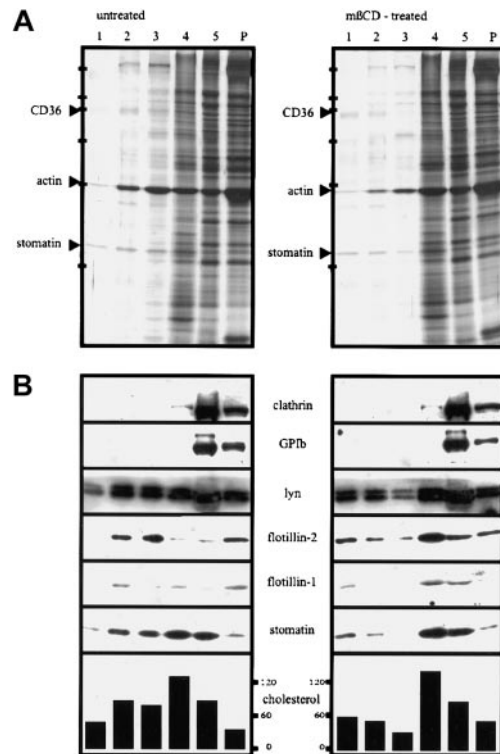

Figure 3. Lipid-raft association of stomatin after TX-100 lysis changes on mβCD-treatment. Platelets (2×10^9 cells/mL) were incubated for 30 minutes at 37°C in the presence (mβCD-treated) or absence (untreated) of 0.5% mβCD, washed twice in buffer I containing 2 mM CaCl$_2$, and lysed in 1% TX-100 at 4°C. The lysates containing 5.3 mg/mL protein were adjusted to 50% sucrose, and 750 μL was transferred to SW 50 centrifuge tubes; overlaid with 40%, 30%, 20%, and 10% sucrose (750 μL each); and centrifuged for 17 hours at 230 000g. Five fractions (750 μL) were collected from the top, and the pellet (P) was resuspended in 750 μL TBS. Aliquots were analyzed by silver staining (A) and Western blotting (B) and for cholesterol content (the concentration of cholesterol is given in nanomoles per milliliter). Equal volumes of the fractions were loaded on the gels except for fraction 5 in panel A, which was diluted 1:10 in sample buffer. Arrowheads in panel A indicate the respective protein bands of fraction 2, which were identified by MALDI-MS. Bars in panel A indicate molecular-weight markers of 205, 116, 97, 66, 45, and 29 kd. Representative data are shown (n = 4).

However, a large amount of stomatin remained in the high-density fractions (fractions 4 and 5), indicating a high solubility in TX-100. Pretreatment of platelets with the cholesterol-depleting agent mβCD resulted in a shift of stomatin, flotillin-1, flotillin-2, and Lyn from the lipid-raft fractions to the high-density fractions (Figure 3B; Western blotting results). As shown by silver staining, the total amount of protein in the raft fractions was reduced compared with that in untreated platelets.

The unusual high solubility of platelet stomatin in TX-100 at 4°C has 2 possible explanations: (1) a large part of stomatin is not present in lipid rafts, (2) stomatin-specific lipid rafts are largely solubilized by TX-100. To address this issue, we tested the solubility of platelet stomatin in different detergents by using stringent centrifugation conditions to recover the membrane skeleton and small lipid rafts in the pellet fraction. Stomatin was predominantly solubilized by NP-40 and TX-100, poorly solubilized by OG, and virtually insoluble in Lubrol and CHAPS (Figure 4). Flotillin-2 was nearly insoluble in all tested detergents except OG. Notably, the mild detergents Lubrol and CHAPS, though chemically quite different, have both been used to isolate specific lipid rafts that would be dissolved in TX-100.[20,41] The insolubility of stomatin in Lubrol and CHAPS therefore suggested a specific association of stomatin with lipid rafts sensitive to TX-100.

We did observe a general TX-100 sensitivity of platelet lipid rafts at low ratios of protein to detergent (< 2 mg/mL; data not shown); however, at 5 mg protein/mL 1% TX-100, stomatin rafts appeared largely soluble, whereas flotillin rafts were stable. Indeed, flotation experiments with CHAPS lysates revealed that virtually all of the stomatin was present in the low-density lipid-raft fraction (Figure 5B). This fraction also contained nearly all of the proteins flotillin-1, flotillin-2, and CD36 and about 50% of the Lyn protein. In contrast, clathrin was detectable only in the high-density soluble and pellet fractions.

The silver stain (Figure 5) showed that a distinct set of proteins was present in the lipid-raft fraction. The strongest bands were analyzed by MALDI-TOF-MS and identified as stomatin, flotillin-1, flotillin-2, CD36, CD9, α_{IIb}, β_3, and GLUT-3. However, in contrast to the results of the flotation experiment with the TX-100 lysate (Figure 3), only minor amounts of actin were present in the lipid-raft fraction, indicating a selective disruption of the cytoskeleton–lipid-raft interaction by CHAPS. These data, together with our finding that stomatin was located mainly at the α-granular membrane, suggest strongly that α granules contain specific lipid rafts that are partly solubilized in TX-100 but stable in CHAPS. In Figure 6, the low-density and high-density fractions from the TX-100 and CHAPS flotation experiments are compared directly, revealing differences in the distribution of specific proteins, particularly CD9 and actin.

Platelet activation results in fusion of the α granules with the plasma membrane and SCCS and release of the granule content. We studied the fate of stomatin in this process. On activation,
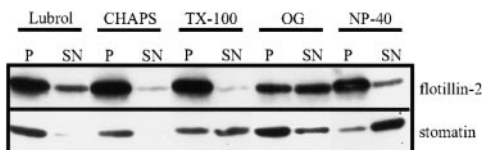

Figure 5. Lipid-raft association of proteins from platelets and α granules after CHAPS lysis. (A,B) Platelets (2 × 10⁹ cells/mL) were lysed in 1% CHAPS at 4°C. The lysates containing 5.0 mg/mL protein were adjusted to 50% sucrose. Then, 750 μL was transferred to SW 50 centrifuge tubes; overlaid with 40%, 30%, 20%, and 10% sucrose (750 μL each); and centrifuged for 17 hours at 230 000g. Five fractions (750 μL) were collected from the top, and the pellet (P) was resuspended in 750 μL TBS. Aliquots were analyzed by silver staining (A) and Western blotting (B) and for cholesterol content (the concentration of cholesterol is given in nanomoles per milliliter). Equal volumes of the fractions were loaded on the gels except for fraction 5 in panel A, which was diluted 1:10 in sample buffer. Arrowheads in panel A indicate the respective protein bands of fraction 2, which were identified by MALDI-MS. Bars in panel A indicate molecular-weight markers of 205, 116, 97, 66, 45, and 29 kd. Representative data are shown (n = 3).

stomatin could be partly recovered in the platelet-free supernatant, suggesting a specific incorporation into microvesicles. Microvesicle release from platelets after activation with strong agonists is a well-described process.[37,42] Platelets were activated with calcium ionophore A23187 (Figure 7A) or thrombin (Figure 7B), and aliquots of the isolated microvesicles and remaining platelets (normalized to protein content) were analyzed by Western
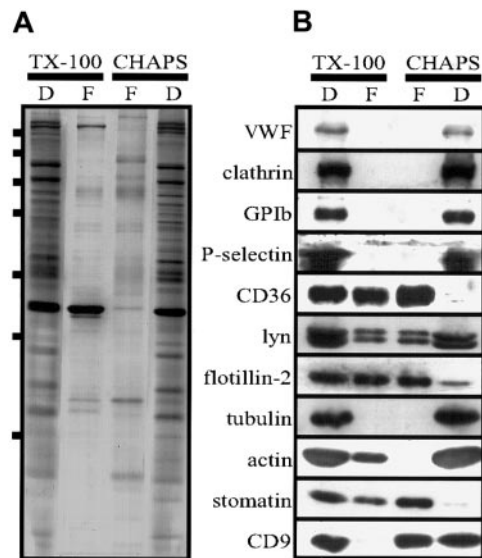
Figure 6. Comparison of lipid rafts isolated from TX-100 and CHAPS lysates. (A,B) Platelets (2 × 10⁹ cells/mL) were lysed in 1% TX-100 or CHAPS at 4°C, and flotation experiments were performed as described in the legends for Figures 3 and 5. Aliquots of the pooled floating (F) fractions 1 to 3 and dense (D) fraction 5 were analyzed. For Western blot analysis (B), equal volumes were loaded on the gel, whereas for silver staining (A), the fraction 5 was diluted 1:30 because of the high protein content. Bars in panel A indicate molecular-weight markers of 250, 150, 100, 75, 50, 37, and 25 kd. Representative data are shown (n = 3).

Figure 4. Detergent solubility of stomatin and flotillin-2. Platelets (2 × 10⁹ cells/mL) were incubated at 4°C with lysis buffer containing 1% of Lubrol, CHAPS, TX-100, NP-40, or 60 mM OG. Insoluble material was formed into pellets (by centrifugation at 100 000g for 1 hour), and equal amounts of the resuspended pellet (P) and the supernatant (SN) were analyzed by SDS-PAGE and Western blotting. Representative data are shown (n = 3).
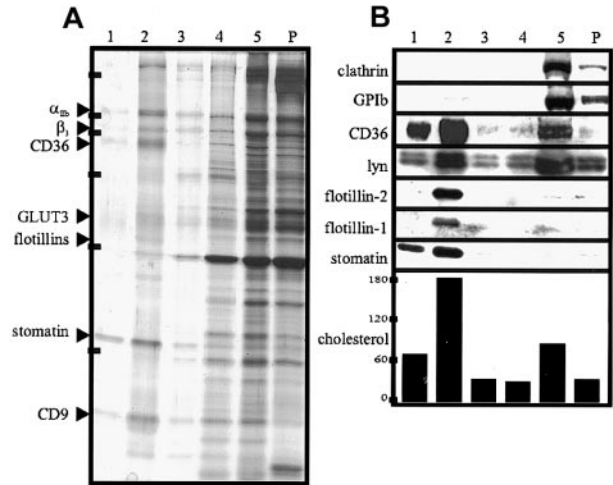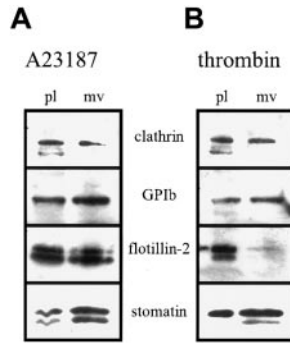
Figure 7. Enrichment of stomatin in microvesicles after platelet activation. Platelets (1 × 10⁹ cells/mL) were activated by incubation with 4 μM ionophore A23187 (A) or 1 U/mL thrombin (B) at 37°C for 30 minutes. Platelets and microvesicles were isolated by differential pelleting steps, and aliquots normalized to equal protein content were analyzed by Western blotting. Representative data are shown (n = 3); pl indicates platelets; and mv, microvesicles.

blotting. In contrast to flotillin-2 and clathrin, stomatin and GPIb were enriched in the microvesicles after A23187 or thrombin activation. Enrichment of GPIb in microvesicles was described previously.[42] Activation with A23187 resulted in cleavage of stomatin and flotillin-2, as indicated by the appearance of double bands on the Western blot (Figure 7). Interestingly, on thrombin activation, the degradation product of stomatin was exclusively present in the microvesicles but not in the remaining platelets. Moreover, flotillin-2 was virtually absent from microvesicles released after thrombin activation.

Activation of platelets is known to result in the activation of proteases and the degradation of several cytoskeletal and membrane proteins.[42-44] We found that degradation of stomatin and flotillin-2 depended on the presence of calcium and could be inhibited by leupeptin, an inhibitor of serine and cysteine proteases (data not shown). More specifically, the membrane-permeable calpain inhibitors E-64d and calpeptin almost completely inhibited stomatin cleavage and significantly reduced the degradation of flotillin-2 and spectrin (Figure 8). In contrast to these proteins, flotillin-1 was not subject to activation-induced degradation. Similar results (data not shown) were obtained when platelets were permeabilized with saponin[45] and incubated with a calpain inhibitor peptide.[46]

Discussion

In this study, we showed that stomatin is an abundant protein constituent of platelets, which had the highest immunocytochemical signal density of all blood cells (Figure 1A). However, in contrast to erythrocytes, in which stomatin is located exclusively at the (plasma) membrane, stomatin in platelets was predominantly localized intracellularly rather than at the cell periphery. Immuno-electron microscopy showed that most of the immunogold labeling was in close proximity to α-granular membranes (Figure 1D). In accordance with this result, analysis of platelet homogenates on sucrose gradients revealed a parallel distribution of stomatin and the α-granular marker proteins P-selectin and VWF (Figure 2). On activation of platelets with calcium ionophore A23187, the immunogold labeling density was increased at the plasma membrane (Figure 1E). This observation supports the proposal that stomatin is present at α granules, since these granules fuse with the plasma membrane on activation.[47]

Subcellular fractionation of platelet organelles revealed that flotillin-1 and flotillin-2 were located predominantly at the platelet plasma membrane or another light membrane, whereas stomatin was associated mainly with α granules (Figure 2). The different localization of these proteins is remarkable because previous studies in erythrocytes revealed that stomatin and the flotillins have similar characteristics as oligomeric lipid-raft proteins.[12] Here, we showed for the first time that these related raft proteins are present in different compartments.

Whereas stomatin was only partly present in lipid rafts, flotillin-2, when isolated after TX-100 solubilization of platelets (Figure 3), was present largely in the low-density fractions of the sucrose gradient. As noted above, the stability of the platelet rafts in TX-100 generally depended on a high ratio of protein to detergent and decreased at concentrations below 2 mg protein/mL TX-100 solution. However, the difference in solubility of stomatin and flotillin-2 at a high protein concentration (5 mg/mL) suggested that these proteins are associated with different types of lipid rafts varying in their degree of TX-100 stability (Figures 3 and 4). About 50% to 70% of flotillin-2 was associated with lipid rafts (Figure 3, lanes 2 and 3), and 30% to 50% was found in the pellet and high-density fraction, indicating a partial association with the cytoskeleton (Figure 3). Pretreatment of platelets with 0.5% mβCD resulted in a shift of stomatin and the flotillins to the high-density fractions of the sucrose density gradient (Figure 3B, lanes 4 and 5), which is a common characteristic of lipid-raft proteins. Pretreatment with 1% mβCD had a more pronounced effect (data not shown). The distribution of cholesterol was also altered after mβCD treatment, with a relative shift from the lipid raft to the soluble pool. This reflects the removal of cholesterol from lipid rafts, a finding in accordance with data from Waheed et al.[48]

In contrast to TX-100, the detergents CHAPS and Lubrol did not solubilize stomatin (Figure 4). We showed that the insolubility of stomatin in CHAPS was due to its association with lipid rafts, since virtually all of the stomatin was present in the low-density fractions (Figure 5, lanes 1 and 2) of the CHAPS flotation assay. Similarly, flotillin-1 and flotillin-2 were found exclusively in the low-density fractions. The altered flotation behavior of stomatin and the flotillins after CHAPS lysis indicates that lipid rafts are more stable in CHAPS than in TX-100 (Figures 3B and 5B). Remarkably, nearly 60% of the total cellular cholesterol was present in the lipid-raft fractions (Figure 5, lanes 1 and 2).
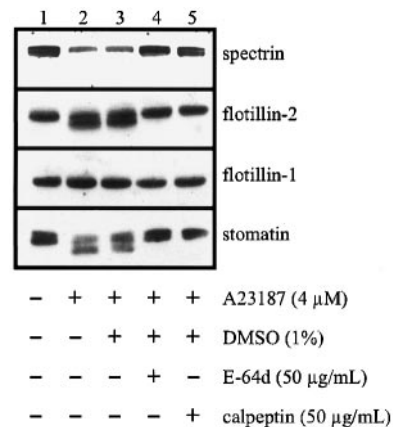

Figure 8. Limited proteolysis of stomatin by calpain after platelet activation. Platelets (1 × 10⁹ cells/mL) were pretreated with the membrane-permeable calpain inhibitors E-64d or calpeptin or with diluent. The platelets were then activated by addition of 4 μM calcium ionophore A23187, and aliquots were analyzed by Western blotting. Representative data are shown (n = 3).

Moreover, it is notable that platelet lipid rafts were generally stable in CHAPS, even at the very low ratio of protein to detergent of 0.6 mg protein/mL detergent solution (data not shown). Simons et al[41] previously showed that neuronal lipid rafts are stable in CHAPS but dissolved in TX-100. The reduction in the amount of lipid-raft–associated actin after CHAPS lysis (compare silver stains shown in Figures 3A, 5A, and 6A and Western blots in 6B) indicates that this detergent disrupts the interaction between the actin cytoskeleton and the lipid rafts.

Apart from stomatin and the flotillin proteins, the major protein components of the CHAPS-insoluble membrane domains were identified as α_{IIb}, β_3, CD36, GLUT-3, and CD9. CD36, the tetraspanin CD9, and the integrin $\alpha_{IIb}\beta_3$ were previously shown to be partly present in platelet lipid rafts after TX-100 lysis.[27] However, a considerably larger pool of CD36 was found to be present in the floating fraction when lysis was done with the mild detergent Brij99 instead of TX-100.[49] Here, we showed that on CHAPS lysis, most of the CD36 was contained in the floating lipid-raft fraction (Figures 5B, 6B), indicating an even higher stability of these rafts in CHAPS than in Brij99. Because CD36 is a major plasma membrane protein and has been shown to be part of one or several multiprotein complexes[49] together with CD9 and $\alpha_{IIb}\beta_3$, we conclude that these complexes are located in lipid rafts at the platelet plasma membrane.

One important conclusion that can be drawn from the flotation experiments and the subcellular localization of stomatin is that the α-granular membrane contains lipid rafts that are partly soluble in TX-100 but stable in CHAPS. We suggest that stomatin could function as an organizer of the α-granular lipid rafts, which might play an important role as platforms for signaling molecules or docking sites for the cytoskeleton during α-granule exocytosis. Whereas the α-granular marker protein P-selectin was not present in lipid rafts (Figure 6B), GLUT-3, the main glucose transporter isoform in platelets, was the only other identified raft protein that is located predominantly on α granules.[50,51] On thrombin stimulation, GLUT-3 translocates to the cell surface and the increased glucose influx meets the high energy demand of platelet plug formation and clot retraction, which is an actomyosin-based process reminiscent of muscle contraction.[50] Interestingly, stomatin interacts with the glucose transporter GLUT-1 in erythrocytes and rat liver cells, thereby exerting some inhibitory function.[52,53] In platelets, stomatin and GLUT-3 might also form a functional protein complex in the α-granular lipid rafts.

We found that lipid rafts of different intracellular membrane origins are recovered in the low-density fraction of the sucrose gradients, thereby showing that careful biochemical and immuno-electron microscopical analyses are necessary to localize the various types of lipid rafts within the complex membrane system of platelets. Different types of lipid rafts in platelets were also suggested by the results of Waheed et al.[48] Moreover, the fact that Lyn is localized predominantly to coated vesicles[33] indicates that these clathrin-coated, endocytic vesicles might also contain lipid rafts. Thus, it remains to be determined whether the flotillin proteins are located at lipid rafts of the plasma membrane, endocytic vesicles, or another platelet organelle. Flotillin-1 was previously identified at different subcellular locations depending on the cell type and state of differentiation. It was originally described as a caveolar protein[25]; however, in neurons[26] and erythrocytes,[12] it is found in noncaveolar rafts at the plasma membrane. In macrophages, flotillin-specific lipid rafts are recruited to the phagosome,[24] whereas in Chinese hamster ovary, PC12, HeLa, and normal rat kidney cells, flotillin-1 is found predominantly in the Golgi complex.[23] Interestingly, on differentiation of PC12 cells, flotillin-1 is relocated to the plasma membrane.[23] The exact subcellular location of the flotillins in platelets remains to be determined; however, the results of our subcellular-fractionation (Figure 2) and detergent-solubility experiments (Figure 4) exclude the possibility that they colocalize with stomatin to α-granular rafts.

Platelets activated by calcium ionophore, thrombin, or collagen release microvesicles, which are thought to exert procoagulant activity at a distance from the site of platelet activation.[37] Microvesicle shedding has been shown to depend on the activity of calpain by cleavage of key cytoskeleton and membrane protein components.[42,54] In contrast to flotillin-1, stomatin and flotillin-2 were cleaved by calpain (Figure 8). However, whereas both flotillin proteins remained predominantly at the platelet plasma membrane after thrombin activation, stomatin became enriched in the released microvesicles (Figure 7). The specific behavior of stomatin and the flotillin proteins in the activation-induced microvesiculation process possibly reflects an underlying mechanism of lipid-raft sorting. Whereas flotillin-specific rafts are excluded from microvesicles, stomatin-specific rafts are sorted specifically into the budding microvesicle. The mechanism of this sorting process and its functional importance remain to be elucidated.

Acknowledgments

References

1. Hiebl-Dirschmied CM, Adolf GR, Prohaska R. Isolation and partial characterization of the human erythrocyte band 7 integral membrane protein. Biochim Biophys Acta. 1991;1065:195-202.

2. Hiebl-Dirschmied CM, Entler B, Glotzmann C, Maurer-Fogy I, Stratowa C, Prohaska R. Cloning and nucleotide sequence of cDNA encoding human erythrocyte band 7 integral membrane protein. Biochim Biophys Acta. 1991;1090:123-124.

3. Wang D, Mentzer WC, Cameron T, Johnson RM. Purification of band 7.2b, a 31-kDa integral phospho-protein absent in hereditary stomatocytosis. J Biol Chem. 1991;266:17826-17831.

4. Stewart GW, Hepworth-Jones BE, Keen JN, Dash BC, Argent AC, Casimir CM. Isolation of cDNA coding for an ubiquitous membrane protein deficient in high Na$^+$, low K$^+$ stomatocytic erythrocytes. Blood. 1992;79:1593-1601.

5. Lande WM, Thiemann PV, Mentzer WC Jr. Missing band 7 membrane protein in two patients with high Na, low K erythrocytes. J Clin Invest. 1982; 70:1273-1280.

6. Stewart GW, Argent AC, Dash BC. Stomatin: a putative cation transport regulator in the red cell membrane. Biochim Biophys Acta. 1993;1225:15-25.

7. Zhu Y, Paszty C, Turetsky T, et al. Stomatocytosis is absent in "stomatin"-deficient murine red blood cells. Blood. 1999;93:2404-2410.

8. Snyers L, Umlauf E, Prohaska R. Oligomeric nature of the integral membrane protein stomatin. J Biol Chem. 1998;273:17221-17226.

9. Snyers L, Umlauf E, Prohaska R. Association of stomatin with lipid-protein complexes in the plasma membrane and the endocytic compartment. Eur J Cell Biol. 1999;78:802-812.

10. Salzer U, Ahorn H, Prohaska R. Identification of the phosphorylation site on human erythrocyte band 7 integral membrane protein: implications for a monotopic protein structure. Biochim Biophys Acta. 1993;1151:149-152.

11. Tavernarakis N, Driscoll M, Kyrpides NC. The SPFH domain: implicated in regulating targeted protein turnover in stomatins and other membrane-associated proteins. Trends Biochem Sci. 1999;24:425-427.

12. Salzer U, Prohaska R. Stomatin, flotillin-1, and flotillin-2 are major integral proteins of erythrocyte lipid rafts. Blood. 2001;97:1141-1143.

13. Simons K, van Meer G. Lipid sorting in epithelial cells. Biochemistry. 1988;27:6197-6202.

14. Simons K, Wandinger-Ness A. Polarized sorting in epithelia. Cell. 1990;62:207-210.

15. Simons K, Ikonen E. Functional rafts in cell membranes. Nature. 1997;387:569-572.

16. Simons K, Toomre D. Lipid rafts and signal transduction. Nat Rev Mol Cell Biol. 2000;1:31-39.

17. Brown DA, London E. Structure and function of sphingolipid- and cholesterol-rich membrane rafts. J Biol Chem. 2000;275:17221-17224.

18. Brown DA, London E. Functions of lipid rafts in biological membranes. Annu Rev Cell Dev Biol. 1998;14:111-136.

19. Schnitzer JE, McIntosh DP, Dvorak AM, Liu J, Oh P. Separation of caveolae from associated microdomains of GPI-anchored proteins. Science. 1995;269:1435-1439.

20. Roper K, Corbeil D, Huttner WB. Retention of prominin in microvilli reveals distinct cholesterol-based lipid micro-domains in the apical plasma membrane. Nat Cell Biol. 2000;2:582-592.

21. Madore N, Smith KL, Graham CH, et al. Functionally different GPI proteins are organized in different domains on the neuronal surface. EMBO J. 1999;18:6917-6926.

22. Gagescu R, Demaurex N, Parton RG, Hunziker W, Huber LA, Gruenberg J. The recycling endosome of Madin-Darby canine kidney cells is a mildly acidic compartment rich in raft components. Mol Biol Cell. 2000;11:2775-2791.

23. Gkantiragas I, Brugger B, Stuven E, et al. Sphingomyelin-enriched microdomains at the golgi complex. Mol Biol Cell. 2001;12:1819-1833.

24. Dermine JF, Duclos S, Garin J, et al. Flotillin-1-enriched lipid raft domains accumulate on maturing phagosomes. J Biol Chem. 2001;276:18507-18512.

25. Bickel PE, Scherer PE, Schnitzer JE, Oh P, Lisanti MP, Lodish HF. Flotillin and epidermal surface antigen define a new family of caveolae-associated integral membrane proteins. J Biol Chem. 1997;272:13793-13802.

26. Lang DM, Lommel S, Jung M, et al. Identification of reggie-1 and reggie-2 as plasma membrane-associated proteins which cocluster with activated GPI-anchored cell adhesion molecules in non-caveolar micropatches in neurons. J Neurobiol. 1998;37:502-523.

27. Dorahy DJ, Lincz LF, Meldrum CJ, Burns GF. Biochemical isolation of a membrane microdomain from resting platelets highly enriched in the plasma membrane glycoprotein CD36. Biochem J. 1996;319:67-72.

28. Dorahy DJ, Burns GF. Active Lyn protein tyrosine kinase is selectively enriched within membrane microdomains of resting platelets. Biochem J. 1998;333:373-379.

29. Berger G, Caen JP, Berndt MC, Cramer EM. Ultrastructural demonstration of CD36 in the α-granule membrane of human platelets and megakaryocytes. Blood. 1993;82:3034-3044.

30. Berger G, Masse JM, Cramer EM. α-granule membrane mirrors the platelet plasma membrane and contains the glycoproteins Ib, IX, and V. Blood. 1996;87:1385-1395.

31. Harrison P, Wilbourn B, Debili N, et al. Uptake of plasma fibrinogen into the α granules of human megakaryocytes and platelets. J Clin Invest. 1989;84:1320-1324.

32. Handagama P, Scarborough RM, Shuman MA, Bainton DF. Endocytosis of fibrinogen into megakaryocyte and platelet α-granules is mediated by αIIb β3 (glycoprotein IIb-IIIa). Blood. 1993;82:135-138.

33. Stenberg PE, Pestina TI, Barrie RJ, Jackson CW. The Src family kinases, Fgr, Fyn, Lck, and Lyn, colocalize with coated membranes in platelets. Blood. 1997;89:2384-2393.

34. Mosgoeller W, Steiner M, Hozak P, Penner E, Wesierska-Gadek J. Nuclear architecture and ultrastructural distribution of poly(ADP-ribosyl) transferase, a multifunctional enzyme. J Cell Sci. 1996;109:409-418.

35. Prendes MJ, Bielek E, Zechmeister-Machhart M, et al. Synthesis and ultrastructural localization of protein C inhibitor in human platelets and megakaryocytes. Blood. 1999;94:1300-1312.

36. Mosgoller W, Schofer C, Derenzini M, Steiner M, Maier U, Wachtler F. Distribution of DNA in human Sertoli cell nucleoli. J Histochem Cytochem. 1993;41:1487-1493.

37. Heijnen HF, Schiel AE, Fijnheer R, Geuze HJ, Sixma JJ. Activated platelets release two types of membrane vesicles: microvesicles by surface shedding and exosomes derived from exocytosis of multivesicular bodies and α-granules. Blood. 1999;94:3791-3799.

38. McGowan EB, Becker E, Detwiler TC. Inhibition of calpain in intact platelets by the thiol protease inhibitor E-64d. Biochem Biophys Res Commun. 1989;158:432-435.

39. Tsujinaka T, Kajiwara Y, Kambayashi J, et al. Synthesis of a new cell penetrating calpain inhibitor (calpeptin). Biochem Biophys Res Commun. 1988;153:1201-1208.

40. Broekman MJ. Homogenization by nitrogen cavitation technique applied to platelet subcellular fractionation. Methods Enzymol. 1992;215:21-32.

41. Simons M, Kramer EM, Thiele C, Stoffel W, Trotter J. Assembly of myelin by association of proteolipid protein with cholesterol- and galactosylceramide-rich membrane domains. J Cell Biol. 2000;151:143-154.

42. Fox JE, Austin CD, Reynolds CC, Steffen PK. Evidence that agonist-induced activation of calpain causes the shedding of procoagulant-containing microvesicles from the membrane of aggregating platelets. J Biol Chem. 1991;266:13289-13295.

43. Earnest JP, Santos GF, Zuerbig S, Fox JE. Dystrophin-related protein in the platelet membrane skeleton. Integrin-induced change in detergent-insolubility and cleavage by calpain in aggregating platelets. J Biol Chem. 1995;270:27259-27265.

44. Oda A, Druker BJ, Ariyoshi H, Smith M, Salzman EW. pp60src is an endogenous substrate for calpain in human blood platelets. J Biol Chem. 1993;268:12603-12608.

45. Scrutton MC, Knight DE, Authi KS. Preparation and uses of semi-permeabilized platelets. In: Watson SP, Authi KS, eds. Platelets. A Practical Approach. Vol 167. Oxford, United Kingdom: Oxford University Press; 1996:47-65.

46. Maki M, Bagci H, Hamaguchi K, Ueda M, Murachi T, Hatanaka M. Inhibition of calpain by a synthetic oligopeptide corresponding to an exon of the human calpastatin gene. J Biol Chem. 1989;264:18866-18869.

47. Reed GL, Fitzgerald ML, Polgar J. Molecular mechanisms of platelet exocytosis: insights into the "secrete" life of thrombocytes. Blood. 2000;96:3334-3342.

48. Waheed AA, Shimada Y, Heijnen HF, et al. Selective binding of perfringolysin O derivative to cholesterol-rich membrane microdomains (rafts). Proc Natl Acad Sci U S A. 2001;98:4926-4931.

49. Miao WM, Vasile E, Lane WS, Lawler J. CD36 associates with CD9 and integrins on human blood platelets. Blood. 2001;97:1689-1696.

50. Heijnen HF, Oorschot V, Sixma JJ, Slot JW, James DE. Thrombin stimulates glucose transport in human platelets via the translocation of the glucose transporter GLUT-3 from α-granules to the cell surface. J Cell Biol. 1997;138:323-330.

51. Sorbara LR, Davies-Hill TM, Koehler-Stec EM, Vannucci SJ, Horne MK, Simpson IA. Thrombin-induced translocation of GLUT3 glucose transporters in human platelets. Biochem J. 1997;328:511-516.

52. Zhang JZ, Hayashi H, Ebina Y, Prohaska R, Ismail-Beigi F. Association of stomatin (band 7.2b) with Glut1 glucose transporter. Arch Biochem Biophys. 1999;372:173-178.

53. Zhang JZ, Abbud W, Prohaska R, Ismail-Beigi F. Overexpression of stomatin depresses GLUT-1 glucose transporter activity. Am J Physiol Cell Physiol. 2001;280:C1277-C1283.

54. Wolf BB, Goldstein JC, Stennicke HR, et al. Calpain functions in a caspase-independent manner to promote apoptosis-like events during platelet activation. Blood. 1999;94:1683-1692.